

Characterization of Silicon Photodiode Detectors with Multilayer Filter Coatings for 17-150 Å

J. F. Seely,^a R. Korde,^b F. Hanser,^c J. Wise,^c G. E. Holland,^d J. Weaver,^e and J. C. Rife^a

^aNaval Research Laboratory, Washington DC 20375

^bInternational Radiation Detectors Inc., 2527 W. 237th Street Unit C, Torrance CA 90505

^cPanametrics Inc., 221 Crescent Street, Waltham MA 02453

^dSFA Inc., 1401 McCormick Drive, Landover MD 20785

^eNRC Postdoctoral Fellow, Naval Research Laboratory, Washington DC 20375

ABSTRACT

Silicon photodiode detectors with multilayer coatings were characterized using synchrotron radiation. The coatings were composed of thin layers of metals and other materials and were designed to provide wavelength bandpasses in the 17-150 Å wavelength region. The measured transmittances of the multilayer coatings are in good agreement with the calculated transmittances. The modeling accounts for the transmittance of the multilayer coating and the deposition of the radiation energy in the underlying silicon photodiode. Detectors with the following layer materials (and wavelength bandpasses) were characterized: Fe/Al (17-30 Å), Mn/Al (19-30 Å), V/Al (24-35 Å), Ti/C (27-40 Å), Pd/Ti (27-50 Å), Ti/Zr/Al (27-50 Å), Ag/CaF₂/Al (36-50 Å), and Ti/Mo/C (50-150 Å).

Keywords: photodiode, soft x-ray, extreme ultraviolet, multilayer coating, filter, detector

1. INTRODUCTION

Silicon photodiode detectors with thin metallic coatings have been developed for the purpose of providing wavelength bandpasses in the extreme ultraviolet and soft x-ray spectral regions.¹ The bandpass is essentially determined by the transmittance of the coating. The coating is deposited on the surface of the photodiode during the photodiode fabrication process at the wafer level. This approach preserves the low noise level of the photodiode detector while providing a robust filter that is superior to a fragile free-standing filter. The sensitivity stability of the coated photodiodes depends primarily on the stability of the layer materials with regard to interdiffusion and redistribution of the layer materials, surface contamination, oxidation, and other possible chemical effects.

Coated photodiode detectors previously have been absolutely calibrated using synchrotron radiation and line emission sources. A photodiode detector with a 3000 Å aluminum coating was used to measure the absolute solar flux in a wavelength bandpass extending from the aluminum L absorption edge at 170 Å to approximately 600 Å.² A photodiode with a beryllium coating was used to measure the absolute emission from laser-produced plasmas in a wavelength range extending from the beryllium K absorption edge at 111 Å to approximately 400 Å.³

In this work, we report the characterization of photodiode detectors with multilayer coatings that establish wavelength bandpasses in the 17-150 Å region. The multilayer coatings are the following: Fe/Al, Mn/Al, V/Al, Ti/C, Pd/Ti, Ti/Zr/Al, Ag/CaF₂/Al, and Ti/Mo/C. For each coating, the last material that is listed is the topmost layer. The sensitivity of each coated photodiode was measured relative to an identical photodiode but having no coating. The measured result is essentially the transmittance of the multilayer coating that establishes the wavelength bandpass of the coated photodiode detector.

The coatings were deposited onto silicon photodiode wafers by Lebow Company, Goleta CA, except for the Ti/Mo/C coating which was deposited by Scientific Coating Laboratory Inc., Santa Clara CA. The layer materials and thicknesses were specified to provide bandpasses in the 17-150 Å wavelength range and to provide good visible light blocking. The photodiodes were of the type AXUV-100G (10x10 mm² sensitive area) or AXUV-96G (6x16 mm² sensitive area). These photodiodes have negligible surface recombination losses, a thin (60 Å) silicon oxide dead layer, and thermal nitridation that provides a stable surface layer.⁴⁻⁷ For wavelengths less than approximately 300 Å, a self-calibration model has been developed for the uncoated photodiodes that does not depend on the use of

a calibration standard.⁸⁻¹⁰ The photodiode efficiency is determined by the optical properties of the photodiode detector and the silicon electron-hole pair creation energy.

2. MEASUREMENT TECHNIQUE

The measurements were performed using the Naval Research Laboratory beamline X24C at the National Synchrotron Light source, Brookhaven National Laboratory. The synchrotron radiation was dispersed by a double-element monochromator that had a resolving power of approximately 600.^{11,12} The wavelength scale was established by the geometry of the monochromator and the absorption edges of beamline filters. The incident radiation was approximately 90% polarized with the electric field vector in the plane of the synchrotron. The photodiode currents were registered by a Keithley Model 617 precision electrometer.

The coated photodiodes were characterized using two different monochromator configurations. The first group of photodiodes, listed in Table 1, were characterized using two 2400 groove/mm gratings in the monochromator. The second group of photodiodes, listed in Table 2, were characterized using a gold mirror and a 600 groove/mm grating in the monochromator. In the latter case, additional beamline filters were utilized to block higher harmonic radiation from the monochromator. The degree of higher harmonic radiation from the monochromator under these two monochromator configurations was previously characterized using transmission gratings and was found to be negligible.

Table 1. Photodiode coatings and measured currents for the first group of photodiodes.

No.	Expected Coating ^a	Modeled Coating ^b	Density (g/cm ³)	Current			
				Room Illumination ^c	Vacuum Illumination ^d	Zero-Order ^e	Dark ^f
1	Uncoated			166 μ A	0.83 μ A	5.5 μ A	10.0 pA
2	4500 \AA Fe 4000 \AA Al	4000 \AA Fe 500 \AA Fe ₂ O ₃ 3900 \AA Al 100 \AA Al ₂ O ₃	7.9 5.2 2.7 4.0	1.7 nA	10.2 pA	-5.1 pA	0.5 pA
3	5000 \AA Mn 5000 \AA Al	5500 \AA Mn 4900 \AA Al 100 \AA Al ₂ O ₃	7.4 2.7 4.0	2.4 nA	21.0 pA	-4.4 pA	1.2 pA
4	6000 \AA V 4000 \AA Al	6500 \AA V 3900 \AA Al 100 \AA Al ₂ O ₃	6.1 2.7 4.0	2.2 nA	20.9 pA	-11.0 pA	0.6 pA
5	5000 \AA Ti 500 \AA C	5500 \AA Ti 300 \AA C	4.5 2.5	1.8 nA	29.3 pA	-11.2 pA	1.1 pA
6	1000 \AA Pd 2000 \AA Ti	800 \AA Pd 3500 \AA Ti 100 \AA C	12.0 4.5 2.5	1.5 nA	25.7 pA	-35.0 pA	1.2 pA

^aExpected layer thicknesses.

^bLayer thicknesses derived from the modeling.

^cCurrent with bright room light illumination.

^dCurrent in vacuum with illumination through a window port.

^eCurrent in vacuum with zero-order monochromator beam illumination (continuum >1100 \AA).

^fCurrent in vacuum with no illumination.

For each photodiode measurement, the top surface (the cathode) of the photodiode was grounded, and the current was registered by the electrometer from the photodiode anode that was electrically isolated from ground. Listed in Table 1 are the photodiode currents measured under various visible-light illumination conditions. Under room illumination conditions (column c), the currents from the uncoated and coated photodiodes were positive. The currents from the coated photodiodes were a factor of 10^5 smaller than the current from the uncoated photodiode. In vacuum ($<5 \times 10^{-7}$ Torr) and when illuminated by visible light through a window port in the vacuum chamber, the currents (column d) from the uncoated and coated photodiodes were positive and lower owing to the weaker illumination.

The size of the beam from the monochromator was approximately $2 \times 2 \text{ mm}^2$. Each photodiode was positioned so that the beam was incident on the center of the photodiode's sensitive area. Column e in Table 1 lists the currents measured when the photodiodes were illuminated by the monochromator's zero diffraction order beam with wavelength $>1100 \text{ \AA}$. The currents from the coated photodiodes are negative and in the range -4.4 pA to -35.0 pA . By comparison, the dark currents are positive and in the range 0.5 pA to 1.2 pA . The small negative currents when the coated photodiodes were illuminated in vacuum by the zero-order monochromator beam are attributed to photoelectrons resulting from radiation absorption near the surfaces of the metal coatings that were collected by the photodiode.¹³

The wavelength of the monochromator was scanned under computer control. Each photodiode was illuminated at the center of the sensitive area by dispersed radiation. The current from each coated photodiode was compared to the current from an identical photodiode but having no coating.

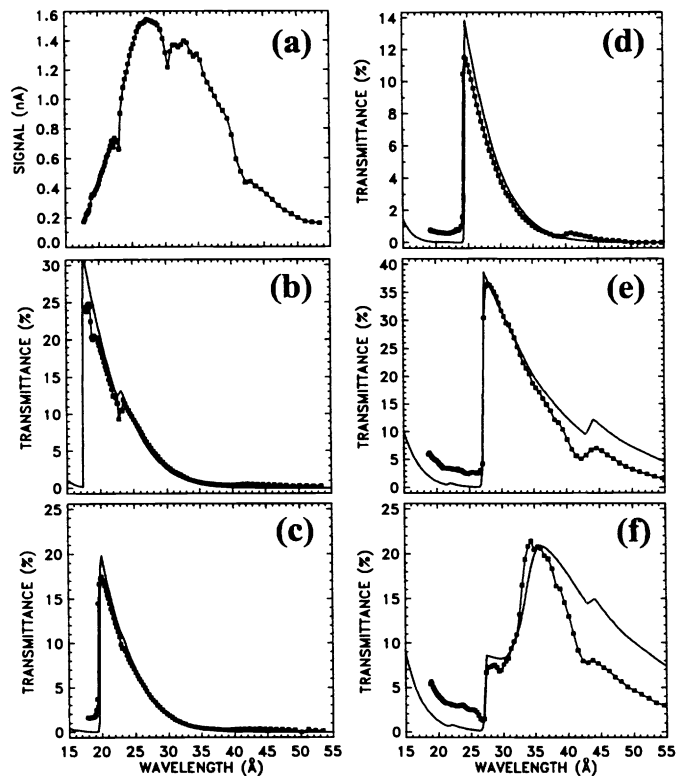


Fig. 1. (a) The current recorded by the uncoated photodiode. The transmittances of the coatings on the coated photodiodes: (b) Fe/Al, (c) Mn/Al, (d) V/Al, (e) Ti/C, and (f) Pd/Ti. The data points are the measured values, and the curves without data points are the calculated transmittances.

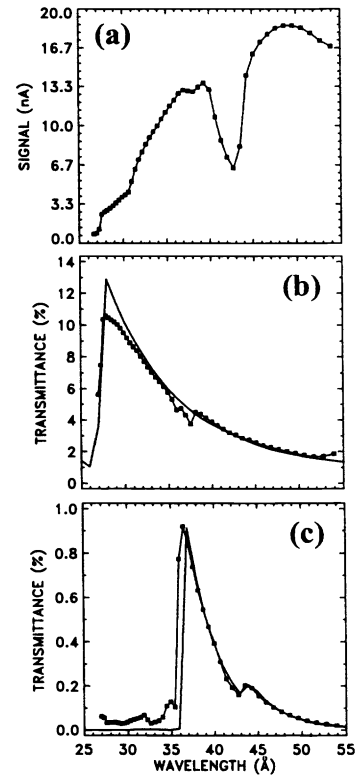


Fig. 2. (a) The current recorded by the uncoated photodiode. The currents recorded by the coated photodiodes: (b) Ti/Zr/Al and (c) Ag/CaF₂/Al. The data points are the measured values, and the curves without data points are the calculated transmittances.

The current from the uncoated photodiode, as a function of wavelength, is shown in Fig. 1(a). Absorption edge features associated with oxygen (at 23.3 Å), nitrogen (31.0 Å), and carbon (43.6 Å) are observed in the current from the uncoated photodiode. The oxygen and nitrogen features result primarily from absorption in the nitrided silicon oxide surface layer of the photodiode. These features are much less prominent in the current recorded by a GaAsP photodiode detector. The carbon absorption feature results primarily from surface contamination on the beamline optics.

The currents from the five coated photodiodes in the first group of photodiodes, divided by the current from the uncoated photodiode, are shown by the curves with data points in Fig. 1(b)-(f). These curves represent the measured effective transmittances of the coatings.

3. EFFECTIVE TRANSMITTANCES OF THE COATINGS

It has been shown that essentially the entire energy of photons that penetrate the 60 Å SiO₂ surface layer of the photodiode is converted to electron-hole pairs in the underlying silicon, and the resulting current is collected by the photodiode's electrode structure.⁴⁻¹⁰ Thus the ratio of the currents collected from the coated and uncoated photodiodes, at a fixed incident photon energy, is directly related to the ratio of the flux penetrating the metal layers and the 60 Å SiO₂ surface layer of the coated photodiode and the flux penetrating the 60 Å SiO₂ surface layer of the uncoated photodiode. This ratio is the effective transmittance of the coating.

The effective transmittances of the coating was calculated using the formalism of Ref. 14. The complex Fresnel coefficients of reflectance and transmittance were calculated at each layer interface. The attenuation in each layer was calculated. The modeled layers included the layers comprising the coating on the photodiode as well as the underlying 60 Å SiO₂ photodiode surface layer. The optical constants were derived from the compilations of Ref. 15 and using the material densities listed in Table 1.

The transmittance of the coated photodiode, calculated in this manner, was divided by the transmittance of the 60 Å SiO₂ surface layer of the uncoated photodiode. The resulting calculated effective transmittances of the first group of coated photodiodes are shown by the curves without data points in Fig. 1(b)-(f). The metal layer thicknesses were adjusted to give the best fit to the data. The expected and modeled layer thicknesses are listed in columns a and b in Table 1, respectively.

For the three photodiodes with an aluminum top layer, the uppermost 100 Å of the aluminum layer was assumed to be Al₂O₃. It was found that the effective transmittances of the Mn/Al, V/Al, and Ti/C photodiodes could be accurately modeled by assuming that the Mn, V, and Ti layers were 500 Å thicker than expected. In addition, the carbon K edge feature in the Ti/C data was fitted by assuming a 300 Å carbon thickness rather than 500 Å.

In order to fit the O K absorption feature in the Fe/Al photodiode data, it was necessary to assume that the Fe layer was partially (11%) oxidized. In the case of the Pd/Ti photodiode, the observed Pd M edge and Ti L edge features determined the Pd and Ti layer thicknesses with values somewhat thinner and thicker than expected, respectively. The C K absorption feature observed for the Pd/Ti photodiode indicated the presence of 100 Å of carbon.

In general, the layer thicknesses (column b in Table 1) determined by the observed spectral features and the modeling are in good agreement with the expected layer thicknesses (column a). The discrepancies may be attributed to inaccuracies in the deposited layer thicknesses and to inaccuracies in the optical constants derived from Ref. 15.

The second group of photodiodes, those characterized using the gold mirror and the 600 groove/mm grating in the monochromator, are listed in Table 2. The Ti/Zr/Al and Ag/CaF₂/Al photodiodes were characterized using a 1600 Å thick titanium beamline filter to attenuate higher harmonic radiation from the monochromator. The current recorded from the uncoated photodiode, shown in Fig. 2(a), has titanium L edge (27.2 Å), nitrogen K edge (31.0 Å), and carbon K edge (43.6 Å) absorption features that are associated with the titanium beamline filter, the photodiode's nitrided silicon oxide surface layer, and carbon contamination on the beamline optics, respectively.

The measured effective transmittance of the Ti/Zr/Al and Ag/CaF₂/Al photodiodes are shown by the curves with data points in Fig. 2(b) and (c). For the Ti/Zr/Al photodiode, the measured data have prominent Zr M_{II} (36.0 Å) and

M_{III} (37.6 Å) absorption features that do not appear in the calculated transmittance. This implies that the Zr optical constants of Ref. 15 do not have accurate Zr M edge data.

Table 2. Photodiode coatings and measured currents for the second group of photodiodes.

No.	Expected Coating ^a	Modeled Coating ^b	Density (g/cm ³)	Current		
				Room Illumination ^c	Zero-Order ^d	Dark ^e
1	Uncoated			68.5 μA	2.0 μA	2.0 pA
2	2500 Å Ti 1000 Å Zr 1000 Å Al	2600 Å Ti 1000 Å Zr 900 Å Al 100 Å Al ₂ O ₃	4.5 6.5 2.7 4.0	3.2 nA	-5.4 pA	0.1 pA
3	2500 Å Ag 10000 Å CaF ₂ 2000 Å Al	2500 Å Ag 11000 Å CaF ₂ 1900 Å Al 100 Å Al ₂ O ₃ 500 Å C	10.5 3.2 2.7 4.0 2.5	1.2 nA	-4.3 pA	1.7 pA
4	Uncoated			64.2 μA	10.9 nA	11.9 pA
5 ^f	500 Å Ti 2000 Å Mo 700 Å C	500 Å Ti 2000 Å Mo 500 Å C	4.5 10.2 2.5	0.14 nA	0.1 pA	0.3 pA
6 ^g	500 Å Ti 2000 Å Mo 700 Å C	500 Å Ti 2000 Å Mo 500 Å C	4.5 10.2 2.5	2.1 nA	0.1 pA	0.5 pA

^aExpected layer thicknesses.

^bLayer thicknesses derived from the modeling.

^cCurrent with room light illumination.

^dCurrent in vacuum with zero-order monochromator beam illumination (continuum >1100 Å).

^eCurrent in vacuum with no illumination.

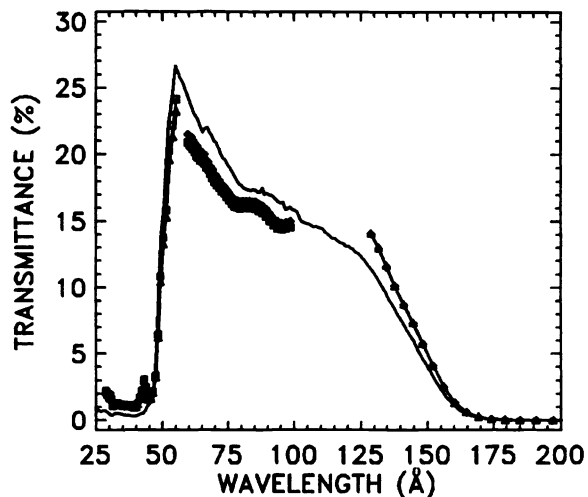
^fUnheated.

^gHeated at a temperature of 155 C for 54 days.

Similarly, the Ag M_{IV} (33.2 Å) and M_V (33.7 Å) edge features that appear in the measured effective transmittance of the Ag/CaF₂/Al photodiode in Fig. 2(c) are not accurately modeled, and the calculated position of the Ca L_{III} edge near 36 Å is inaccurate. The C K absorption feature in the measured effective transmittance of the Ag/CaF₂/Al photodiode indicated a 500 Å thickness of carbon that was unexpected.

Two Ti/Mo/C photodiodes were characterized. One was heated to a temperature of 155 C for a period of 54 days, and the other was unheated. These photodiodes were characterized using the gold mirror and the 600 groove/mm grating in the monochromator. Data were recorded in three wavelength regions using titanium, boron, and silicon beamline filters. The measured effective transmittances of the two Ti/Mo/C photodiodes are shown in Fig. 3 by the data points. The measurements are practically identical within the uncertainties of the measurements. This implies that the heat treatment did not significantly affect the effective transmittance of the Ti/Mo/C coating. The curve in Fig. 3 without data points is the calculated transmittance. The calculation disagrees with the measurements in some wavelength regions. This disagreement may result from inaccurate optical constants for Ti, Mo, and C in these wavelength regions, or from a change in the optical constants resulting from the mixing of Ti, Mo, and C. The

Fig. 3. The transmittances of the coatings on the unheated and heated Ti/Mo/C photodiodes. The data points are the measured values, and the curve without data points is the calculation.



disagreement between the measured and calculated transmittance of the Ti/Mo/C coating will require further studies to resolve.

4. CONCLUSIONS

The effective transmittances of metal coatings on silicon photodiodes were measured using synchrotron radiation in the 17-150 Å wavelength region. Based on the modeling of the effective transmittances using tabulated optical constants, it was found that small adjustments to the expected layer thicknesses had to be made to achieve good agreement with the measured transmittances. In addition, for some of the coated photodiodes, the observed spectral features and the modeling indicated a small but significant degree of oxidation and carbon contamination.

In general, this work demonstrates that it is possible to design and deposit metal coatings on silicon photodiodes that have bandpasses in the 17-150 Å wavelength region. The precision of the design of the transmittance bandpasses will be improved as empirical experience is gained regarding the stability of the layer materials. It may be possible to design and fabricate coated photodiodes that function as a Ross filter set, where the signals recorded by photodiodes with different coatings are subtracted to isolate the signal in narrow wavelength bandpasses of interest.¹⁶

A similar study of coated photodiodes with bandpasses at longer wavelengths, up to 1200 Å, is in progress. Those coated photodiodes will be deployed on the next series of GOES spacecraft to record the absolute solar x-ray flux dispersed by free-standing transmission gratings.

5. ACKNOWLEDGEMENTS

Part of the work was done at the National Synchrotron Light Source, which is sponsored by the Department of Energy under contract DEAC02-76CH00016.

6. REFERENCES

1. L. R. Canfield, R. Vest, T. N. Woods, and R. Korde, "Silicon photodiodes with integrated thin film filters for selective bandpasses in the extreme ultraviolet," *Ultraviolet Technology V*, SPIE **2282**, 31-38 (1994).
2. H. S. Ogawa, L. R. Canfield, D. McMullin, and D. L. Judge, "Sounding rocket measurement of the absolute solar EUV flux utilizing a silicon photodiode," *J. Geophys. Res.* **95**, 4291-4295 (1990).
3. R. L. Kauffman, D. W. Phillips, and R. C. Spitzer, "X-ray production ~13 nm from laser-produced plasmas for projection x-ray lithography applications," *Appl. Opt.* **32**, 6897-6900 (1993).
4. L. R. Canfield, "Photodiode Detectors," in *Vacuum Ultraviolet Spectroscopy II*, ed. by J. A. R. Samson and D. L. Ederer (Academic Press, San Diego, 1998).

5. R. Korde and J. Geist, "Stable, high quantum efficiency UV-enhanced silicon photodiodes by arsenic diffusion," *Solid State Electronics* **30**, 89-92 (1987).
6. L. R. Canfield, J. Kerner, and R. Korde, "Stability and quantum efficiency performance of silicon photodiode detectors in the far ultraviolet," *Appl. Opt.* **28**, 3940-3943 (1989).
7. R. Korde, J. S. Cable, and L. R. Canfield, "One gigarad passivating nitrided oxides for 100% internal quantum efficiency silicon photodiodes," *IEEE Trans. Nucl. Science* **40**, 1655-1659 (1993).
8. M. Krumrey and E. Tegeler, "Self-calibration of semiconductor photodiodes in the soft x-ray region," *Rev. Sc. Instrum.* **63**, 797-801 (1992).
9. F. Scholze, H. Rabus, and G. Ulm, "Measurement of the mean electron-hole pair creation energy in crystalline silicon for photons in the 50-1500 eV spectral range," *Appl. Phys. Lett.* **69**, 2974-2976 (1996).
10. E. M. Gullikson, R. Korde, L. R. Canfield, and R. E. Vest, "Stable silicon photodiodes for absolute intensity measurements in the VUV and soft x-ray regions," *J. Electron Spectr. Related Phenomena* **80**, 313-316 (1996).
11. J. C. Rife, H. R. Sadeghi, and W. R. Hunter, "Upgrades and recent performance of the grating/crystal monochromator," *Rev. Sci. Instrum.* **60**, 2064-2067 (1989).
12. W. R. Hunter and J. C. Rife, "An ultrahigh vacuum reflectometer/goniometer for use with synchrotron radiation," *Nucl. Instrum. Methods* **A246**, 465-468 (1986).
13. R. E. Vest and L. R. Canfield, "Photoemission from silicon photodiodes and induced changes in the detection efficiency in the far ultraviolet," *AIP Conf. Proc.*, vol. **417**, 234-240 (1997).
14. R. F. Potter, "Basic parameters for measuring optical properties," in *Handbook of Optical Constants of Solids*, ed. By E. D. Palik (Academic Press, 1985), page 16.
15. B. L. Henke, E. M. Gullikson, and J. C. Davis, "X-ray interactions: photoabsorption, scattering, transmission, and reflection at E=50-30,000 eV, Z=1-92," *At. Data Nucl. Data Tables* **54**, 181-342 (1993). Updated optical constants were obtained from the internet site cindy.lbl.gov/optical_constants.
16. L. Marrelli, P. Martin, and A. Murari, "Development and tests of a simple multifoil spectrometer for highly time-resolved line intensity measurements in the RFX experiment," *Meas. Sci. Technol.* **6**, 1690-1698 (1995).